Title

A Strategy for Direct Chemical Activation of the Retinoblastoma Protein

Journal

ACS Chemical Biology, 11(5)

ISSN

1554-8929

Authors

Pye, Cameron R
Bray, Walter M
Brown, Elise R
et al.

Publication Date

2016-05-20

DOI

10.1021/acschembio.6b00011

Peer reviewed

ACS chemical biology

Letters

pubs.acs.org/acschemicalbiology

A Strategy for Direct Chemical Activation of the Retinoblastoma Protein

Cameron R. Pye, Walter M. Bray, Elise R. Brown, Jason R. Burke, R. Scott Lokey, and Seth M. Rubin*

Department of Chemistry and Biochemistry, University of California, Santa Cruz, California 95064, United States

Supporting Information

ABSTRACT: The retinoblastoma (Rb) tumor suppressor protein negatively regulates cell proliferation by binding and inhibiting E2F transcription factors. Rb inactivation occurs in cancer cells upon cyclin-dependent kinase (Cdk) phosphorylation, which induces E2F release and activation of cell cycle genes. We present a strategy for activating phosphorylated Rb with molecules that bind Rb directly and enhance affinity for E2F. We developed a fluorescence polarization assay that can detect the effect of exogenous compounds on modulating affinity of Rb for the E2F transactivation domain. We found that a peptide capable of disrupting the compact inactive Rb conformation increases affinity of the repressive Rb−E2F complex. Our results demonstrate the feasibility of discovering novel molecules that target the cell cycle and proliferation through directly targeting Rb rather than upstream kinase activity.

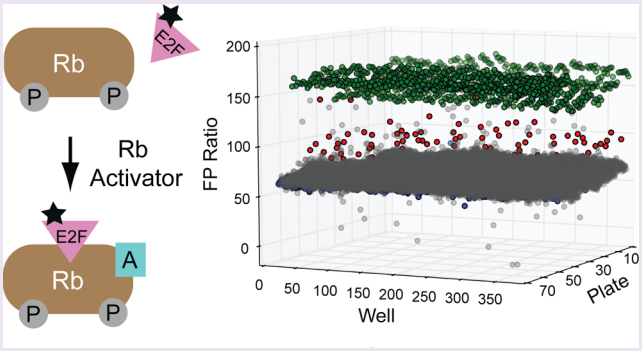

Rb regulates proliferation through controlling the cell cycle, differentiation, senescence, and cell survival.[1−4] Rb orchestrates proper cellular signals with the mechanics of cell cycle progression, and cancer cells almost invariably have alterations in Rb pathway components that enable uncontrolled cell proliferation.[1,2,4−7] While deletion of the gene and full loss of the Rb protein is observed in some cancers, in the vast majority of cases, Rb pathway inactivation in cancer cells is achieved through activation of cyclin/Cdk complexes or inactivation of proteins that inhibit Cdk activity.[2,5,7] Thus, chemotherapeutic strategies that directly promote Rb activity would be relevant to most tumors.

We describe here a novel approach to reversing Rb inactivation with molecules that directly bind Rb itself. There are potential therapeutic advantages to such compounds over current Cdk inhibitors, including potency and specificity.[8] In addition, the specificity of such molecules would give them unprecedented advantages for studying the Rb pathway and its role in tumor suppression. For example, currently the only chemical approach to preventing Rb inactivation is through Cdk inhibition, which has off-target effects from preventing phosphorylation of other substrates.[8] Despite these motivations, no direct chemical probes of Rb exist beyond molecules that specifically inhibit Rb association with viral oncoproteins.[9]

Rb arrests cells largely due to its ability to repress E2F-mediated gene expression.[3] Rb binds E2F primarily through an association of its so-called "pocket" domain with the E2F transactivation domain ($E2F^{TD}$). $E2F^{TD}$ binding by the pocket is necessary for Rb activity in growth suppression, cell cycle control, and E2F inhibition.[3] The Rb pocket domain has an additional protein interaction cleft known as the "LxCxE" site, which binds oncogenic viral proteins and cellular proteins containing the LxCxExϕ sequence motif (ϕ is a hydrophobic residue).[3,10] Several specific Cdk phosphorylation events inhibit E2F binding upon S phase entry,[11,12] however Thr373 phosphorylation has the most pronounced effect in quantitative *in vitro* assays.[13,14] Evidence also suggests that Thr373 phosphorylation is the most critical event for Rb inactivation *in vivo*. Thr373 is the only phosphorylation site sufficient for Cdk-induced inactivation of Rb in cells, and mutation of Thr373 significantly inhibits Cdk-induced Rb−E2F dissociation and E2F activation.[15−17]

We set out to identify molecules that directly activate Rb by stabilizing the association of $E2F^{TD}$ with Cdk-phosphorylated Rb. To search for such compounds, we crafted a fluorescence polarization assay that is amenable to high throughput screening. An $E2F^{TD}$ peptide (human E2F2 amino acids 409−428) was synthesized with a tetramethylrhodamine dye (TMR) at its N-terminus ($E2F^{TMR}$). We assayed binding of $E2F^{TMR}$ to an Rb protein construct (Rb^{NP}) that contains the Rb N-terminal domain (RbN) and pocket domain but lacks internal loops in each domain (residues 55−787, Δ245−267, Δ582−642).[14] This minimized Rb construct contains two phosphorylation sites (T356 and T373) and the structural elements necessary and sufficient for recapitulating the inhibitory effect of T373 phosphorylation on $E2F^{TD}$ binding.[14]

We assayed fluorescence polarization (FP) ratios in 384-well format using 10 nM $E2F^{TMR}$ (Figure 1a). The FP ratio for free $E2F^{TMR}$ is ∼20 in our assay conditions, and the FP ratio

Received: January 6, 2016
Accepted: February 4, 2016
Published: February 4, 2016

   DOI: 10.1021/acschembio.6b00011

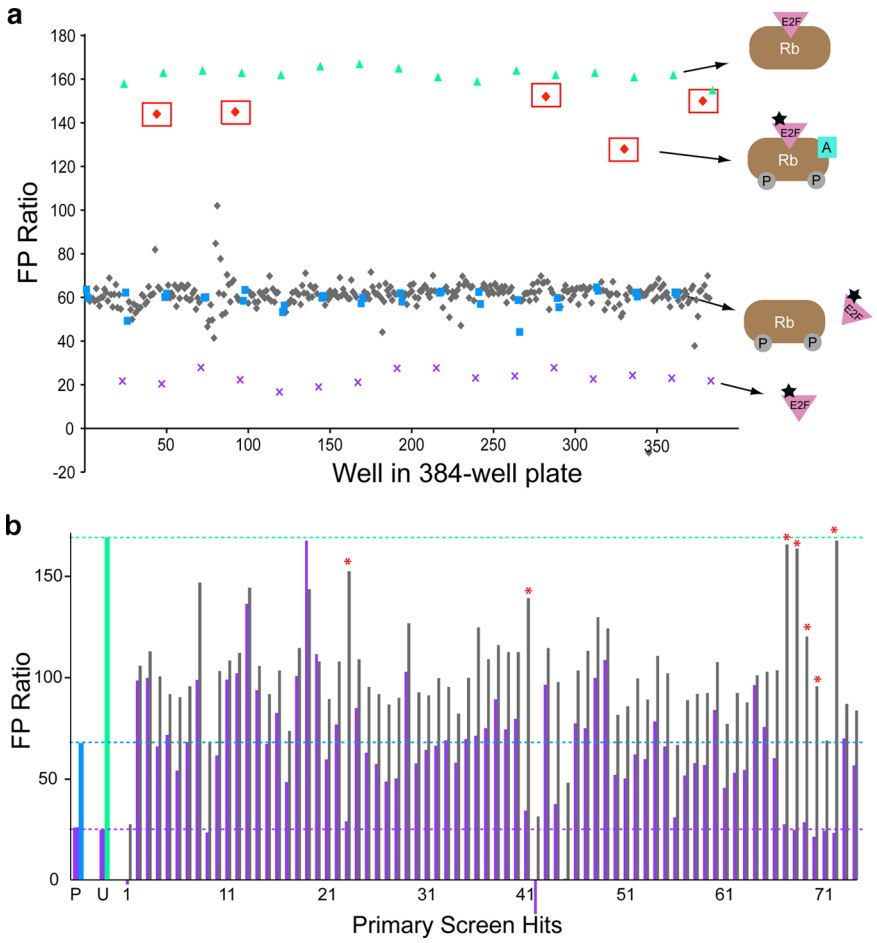

Figure 1. Fluorescence polarization screen for enhancers of Rb−E2F binding. (a) Sample data from the primary screen. FP ratio is plotted for each well in a 384-well plate. The wells contain phosphorylated Rb^{NP} and compounds (gray diamonds) or DMSO (blue squares, "negative control"), unphosphorylated Rb^{NP} (green triangles, "positive control"), or free $E2F^{TMR}$ alone (purple crosses). The boxed red diamonds are hits that increase the FP ratio of $E2F^{TMR}$ in the presence of phosphorylated Rb^{NP}. (b) Follow-up assay in which the effect of the compounds on $E2F^{TMR}$ FP ratio was determined in the absence (purple bars) and presence (gray bars) of phosphorylated Rb^{NP}. The phosphorylated Rb^{NP} negative (P, blue bar) and unphosphorylated Rb^{NP} (U, green bar) positive controls are shown on the left. Hits were validated (red asterisks) if they yielded low FP ratios similar to controls in the Rb^{NP} target-minus (dashed purple line) assay and high FP ratios in the Rb^{NP} target-positive assay (dashed green line).

increases upon addition of 10 nM phosphorylated Rb^{NP} and 10 nM unphosphorylated Rb^{NP} to ∼60 and ∼165, respectively. The more modest FP ratio increase upon addition of phosphorylated Rb^{NP} reflects its approximately 10-fold weaker affinity for $E2F^{TMR}$ compared to the affinity of unphosphorylated Rb^{NP} for $E2F^{TMR}$.[14] We conducted a pilot screen using a 21 120 small molecule library from ChemDiv that contains groups of analogs based on ∼1200 structurally diverse "drug-like" scaffolds. Fifty μM of each compound was incubated with 20 nM phosphorylated Rb^{NP}, and then 10 nM $E2F^{TMR}$ was added. Control wells were used that had no protein ($E2F^{TMR}$-only) or had 0.5% (by volume) DMSO added to either unphosphorylated or phosphorylated Rb^{NP}.

Sample data from one 384-well plate are shown in Figure 1a, and results for the entire screen can be seen in Supporting Figure S1. We looked for hit compounds that raised the FP ratio toward that of unphosphorylated, tighter-binding Rb^{NP}. In this primary screen, the assay had an average $Z' = 0.82 \pm 0.02$.[18] 74 compounds were selected as hits (0.35% hit rate) that had FP ratios higher than the average FP of phosphorylated Rb^{NP} with B-scores[19] of 10 (Z-score of 7.7) or higher. These hits also satisfied the criterion that the measured overall fluorescence intensity was less than three standard deviations above average control fluorescence intensity.

We recognized that because we are seeking compounds that increase the FP ratio, which reflects enhanced Rb binding, a molecule that induces $E2F^{TMR}$ aggregation would be detected in the screen as a hit.[20] To rule out these false-positives, we tested screen hits in a follow-up "target-minus" assay in which phosphorylated Rb^{NP} was left out (Figure 1b). Most of the initial hits resulted in a perturbed FP ratio in the absence of a target, likely the result of either intrinsic fluorescence or compound induced aggregation of the TMR-peptide. We did find seven hits in the library that induced no effect in the absence of Rb^{NP} and enhanced the FP ratio in the presence of phosphorylated Rb^{NP} (red asterisks in Figure 1b and Supporting Information Table). Four of the seven compounds increased the affinity of $E2F^{TMR}$ for phosphorylated Rb^{NP} in a complete protein titration (Supporting Information Figure S2). Those four validated hits contain a common core scaffold based on 1,6-dimethylpyrimido[5,4-*e*][1,2,4]triazene-5,7(1H,6H)-dione. Such triazene compounds are known to generate reactive oxygen species (ROS) that may induce off-target effects in cells.[21] We found that triazene compound activity in

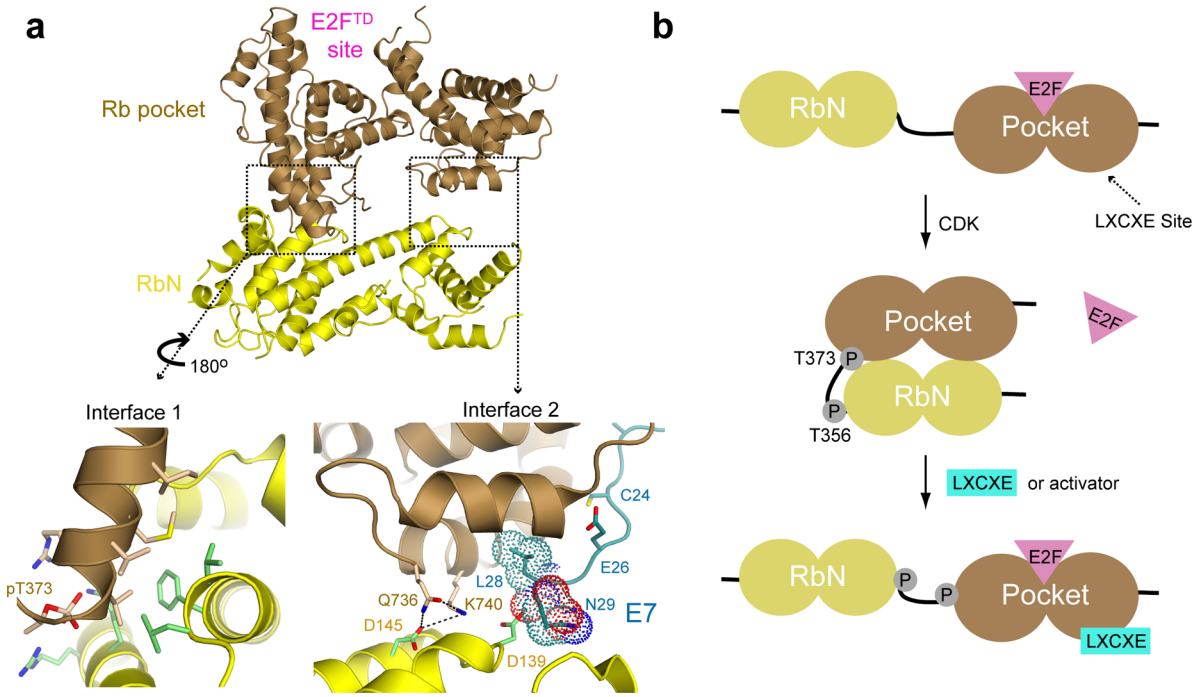

Figure 2. Structure-based strategy for activation of Rb. (a) Structure of phosphorylated Rb (from PDB code: 4ELJ). Docking between the Rb N-terminal domain (RbN, yellow) and the pocket domain (brown) occurs across two interfaces. Interface 1 is mediated by a pocket helix that is nucleated by Thr373 phosphorylation. Interface 2 is near the LxCxE-binding cleft in the pocket. The E7 peptide (cyan backbone), which is shown bound at its site in the unphosphorylated pocket (from PDB code: 1GUX), clashes with RbN residue Asp139 at the interface. (b) Phosphorylation of sites in the Rb interdomain linker induces a conformational change that allosterically inhibits $E2F^{TD}$ binding. We find that an LxCxE peptide acts as an activator by binding Rb and inhibiting the RbN-pocket interdomain association.

the FP assay was lost in the presence of catalase (not shown), so we did not pursue them further.

We next explored a strategy for developing Rb activators that are motivated by the structural mechanism underlying how the Rb−$E2F^{TD}$ complex is inhibited by Rb phosphorylation (Figure 2).[14] Thr373 phosphorylation induces an interdomain association between RbN and the pocket, which allosterically opens the $E2F^{TD}$ binding cleft to weaken affinity. RbN-pocket association occurs across two interfaces (Figure 2a), both of which must be formed to open up the $E2F^{TD}$-binding site and disrupt interactions between the pocket and $E2F^{TD}$. One interface is anchored by the first helix of the pocket domain, which is nucleated by Thr373 phosphorylation and docks into a hydrophobic groove in RbN. The RbN position at the second interface is close to the LxCxE binding site in the pocket domain (see for example the structure of the human papilloma virus (HPV) E7 LxCxE peptide-pocket domain complex).[10,14] From a structural alignment (Figure 2a), the binding of the LxCxE peptide and interdomain docking appear incompatible.

We reasoned that molecules that inhibit interdomain docking would stabilize $E2F^{TD}$ binding to phosphorylated Rb by preventing the allosteric opening of the E2F binding site (Figure 2b). Moreover, because the LxCxE peptide binds near the second RbN-pocket interface (interface 2 in Figure 2a), we hypothesized that the LxCxE peptide would disrupt docking and act as an activator. We tested the effects of the LxCxE peptide from the HPV E7 protein on $E2F^{TMR}$ binding to Rb^{NP} using the FP assay as in the pilot screen but using a full protein titration (Figure 3a). The affinity of $E2F^{TMR}$ for unphosphorylated Rb^{NP} (K_d = 4.3 ± 0.2 nM) is 8-fold tighter than its affinity for phosphorylated Rb^{NP} (K_d = 31 ± 4 nM). In the presence of 10 μM E7 LxCxE peptide, phosphorylated Rb^{NP} binds $E2F^{TMR}$ with 2-fold higher affinity (K_d = 16 ± 2 nM), which implicates the LxCxE peptide as an example of a desired Rb activator molecule. In the presence of 2 μM full length E7 protein, $E2F^{TMR}$ binds phosphorylated Rb^{NP} even tighter (K_d = 4.6 ± 0.3 nM) and with similar affinity as unphosphorylated Rb^{NP}.

We found that the LxCxE peptide and full-length E7 increased Rb^{NP}−$E2F^{TMR}$ affinity with EC_{50} = 190 ± 40 nM and EC_{50} = 10 ± 2 nM, respectively (Figure 3b). The greater potency of the full-length protein correlates with its known 20-fold greater affinity for the Rb pocket domain.[22] We suggest that the greater highest activity of the E7 protein (~100%) compared to the LxCxE peptide (~70%) may result from the fact that its larger size is better suited for occluding the RbN-pocket interface. We found that the LxCxE-peptide and E7 protein do not affect $E2F^{TD}$ binding to Rb if the docking interface is mutated (Q736A/K740A; Supporting Information Figure 3), which supports further our proposal that these activators function by disrupting interdomain docking. We also tested two LxCxE-like peptides from cyclin D (no hydrophobic in +2 position) and LIN52 (LxSxE), which have weak affinity for Rb.[23] These variant peptides and a compound previously reported to bind the LxCxE cleft (compound #478337 from Fera et al.[9]) show no effect in the Rb activation assay (Figure 3b).

To confirm the stabilizing effect of the LxCxE peptide in an orthogonal assay, we measured affinities using isothermal titration calorimetry (Figure 4). We found that $E2F1^{TD}$ binds unphosphorylated Rb^{NP} with similar affinity in the absence (K_d = 70 ± 20 nM) and presence (K_d = 110 ± 20 nM) of excess E7 LxCxE peptide (Figure 4a). In contrast, the affinity of $E2F1^{TD}$ for phosphorylated Rb^{NP} is enhanced in the presence of LxCxE peptide (K_d = 340 ± 20 nM) compared to in its absence (K_d =

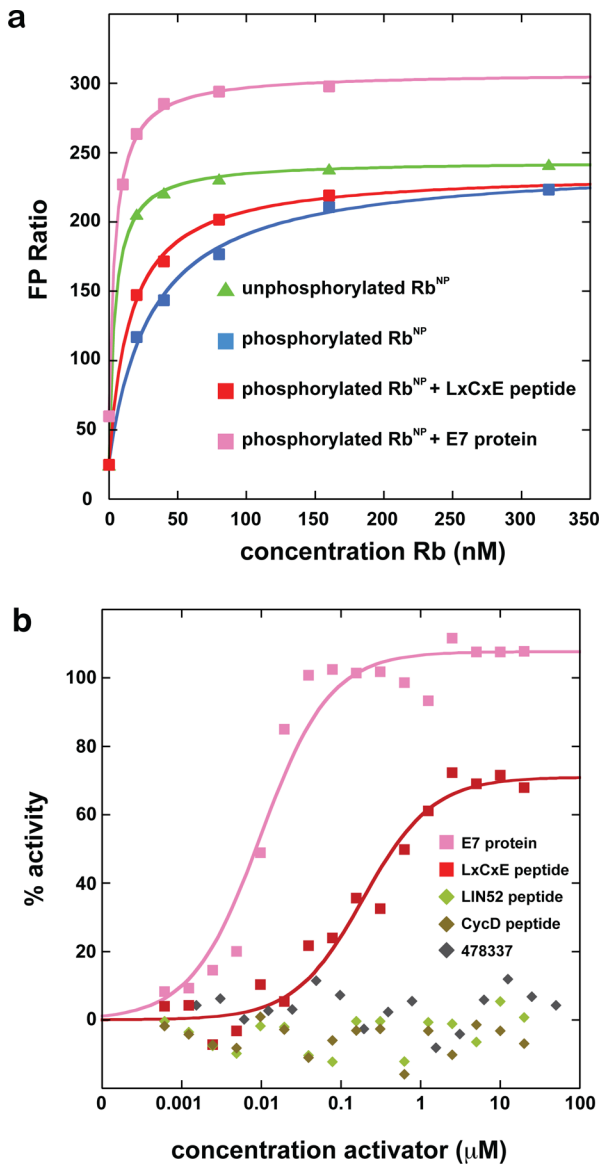

Figure 3. LxCxE peptide shown to act as an Rb activator. (a) Titration of unphosphorylated and phosphorylated Rb^{NP} into $E2F^{TMR}$. In the presence of the E7 LxCxE peptide and full-length E7 protein, the affinity is increased. (b) EC50 measurements of LxCxE peptide and E7 protein activity. Compound #478337 from Fera *et al.*[9] and LxCxE variant peptides from cyclin D and LIN52 do not show activity.

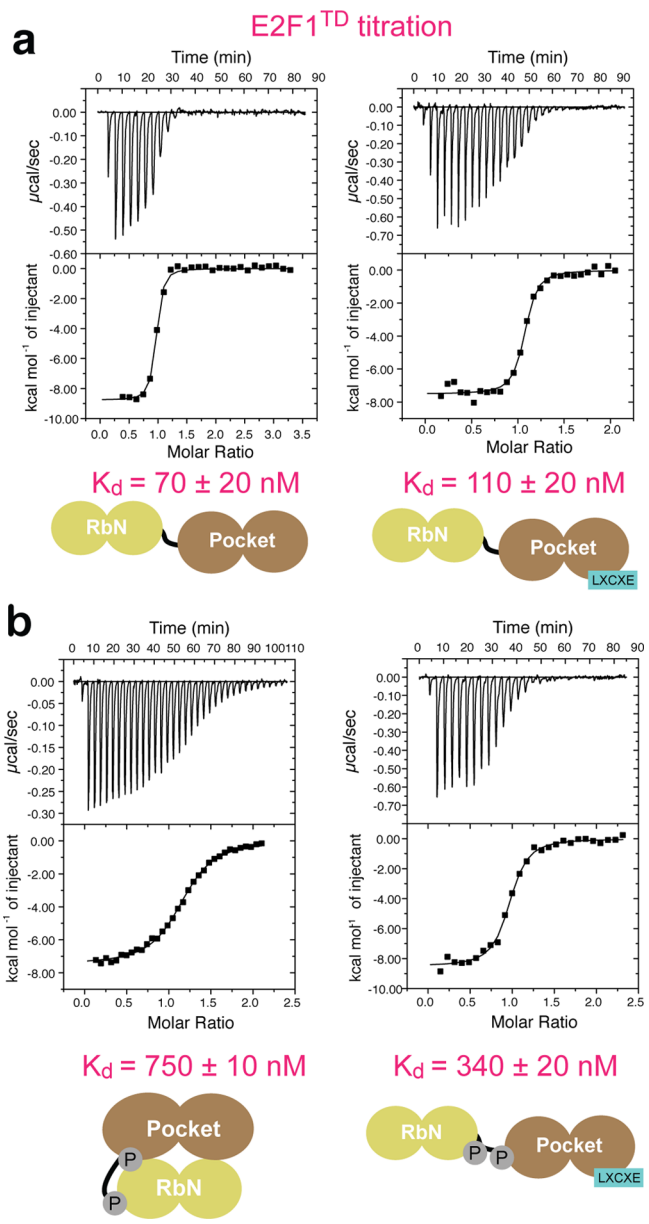

Figure 4. The E7 LxCxE peptide increases affinity of $E2F^{TD}$ for phosphorylated Rb. Representative ITC curves and average K_d measurements are shown for $E2F1^{TD}$ titration into unphosphorylated (a) and phosphorylated (b) Rb^{NP}.

750 ± 10 nM; Figure 4b). The observed increase in affinity that is specific for phosphorylated Rb demonstrates that molecules that interfere with the structural changes induced by Rb phosphorylation can act as Rb activators. We note that while the fold-change due to the LxCxE peptide is similar in the ITC assay as in the FP assay, measured Rb^{NP}–E2F affinities are greater using FP, perhaps due to the hydrophobic TMR dye.

In conclusion, we have developed a robust fluorescence polarization assay for screening molecules that modulate the binding between Rb and E2F, and we found that an LxCxE peptide from the HPV E7 protein, which is known to bind at the RbN-pocket interface,[10,14] increases affinity of the complex. Several observations support the idea that isolated LxCxE peptides or derivatives could be used as Rb–E2F stabilizers in cells. While the E7 and related viral oncoproteins disrupt Rb–E2F complexes in cells to stimulate proliferation, in each case the LxCxE-containing domain is insufficient. Additional domains that directly inhibit Rb–E2F association are required, and in the case of E7, the additional domain targets binding of the Rb C-terminal domain to E2F.[24−26] Notably, expression of an SV40 virus T-antigen protein mutant, which contains the LxCxE motif but lacks the Rb–E2F dissociating domain, enhances the population of Rb–E2F complexes relative to free E2F in fibroblast cells.[26] Moreover, the fact that T373 mutation inhibits Rb–E2F dissociation and E2F activation in cells[15−17] suggests that the affinity increase achieved here, which negates the effect of T373 phosphorylation, may effectively modulate Rb activity *in vivo*.

While the E7 LxCxE peptide is effective *in vitro*, its likely poor pharmacokinetic properties and extended binding structure make it a suboptimal lead for a therapeutic or chemical probe. However, we envision developing peptide

mimics that circumvent these shortcomings such as stapled or cyclic peptides. A group of thiadiazolidinedione compounds has been reported to competitively inhibit Rb-LxCxE association.[9] In an experiment with one such compound reported to bind Rb with 200 nM affinity (#478337 in Fera et al.[9]), we did not observe any effect on $E2F^{TD}$ affinity for phosphorylated Rb^{NP} (Figure 3b). It may be that the specific molecular requirements of inhibiting viral protein LxCxE binding to the pocket cleft and disrupting the RbN-pocket interdomain docking are distinct. Indeed, the location of the LxCxE peptide-binding site is adjacent to but not directly overlapping the interdomain interface (Figure 2a). The full-length E7 protein may be a more effective activator than the peptide (Figure 3) because additional interactions occlude this interface. We propose that LxCxExL peptide derivatives may be more active if they are extended at their C-terminus to overlap more extensively with the RbN docking surface in the pocket. As seen in Figure 2a, N29 (in the +1 position relative to the second L in the LxCxExL motif) clashes with RbN, and addition of optimized chemical groups at this end may impinge more on pocket−RbN interactions. With respect to further screening, our results suggest that libraries containing compounds with larger scaffolds, such as natural products derived libraries, may be more suitable for producing lead activators. We anticipate that ideal compounds would access the hydrophobic pocket bound by the second leucine in the "LxCxExL" peptide and also contact the Gln736/Lys740 surface that forms the docking interface (Figure 2a).

In addition to the molecules discussed here, we propose developing Rb activators that bind the RbN groove forming the primary RbN-pocket interface (interface 1 in Figure 2a). By inhibiting docking of the phosphorylated pocket helix, these molecules may stabilize $E2F^{TD}$ binding to phosphorylated Rb as desired. The pocket helix contacts the groove using hydrophobic residues along one face of an amphipathic helix. This type of interaction has been successfully targeted by small molecules.[27−30] A classic example is the p53−MDM2 interface, formed by residues in the *i*, *i* + 4, and *i* + 7 positions of a p53 helix, for which *cis*-imadazoline (Nutlin) and spiro-oxindole (MI-219) inhibitors have been found.[29,30] Therefore, while our screen results suggest that disrupting the RbN-pocket association is a challenge for small molecules, recent successes in protein−protein interaction inhibition suggest the promise of finding a lead compound for direct Rb activation.

METHODS

Protein and Peptide Reagents. Rb^{NP} and $E2F1^{TD}$ (E2F1 residues 409−426) were expressed in *E. coli* as GST-fusion proteins and purified with GS4B sepharose as previously described.[14] Following elution from the affinity resin, the fusion protein was diluted 3-fold into a buffer containing 25 mM Tris and 1 mM DTT (pH 8.0). Protein was then loaded onto a Source Q ion exchange column equilibrated in the same low salt buffer and eluted from the column in a gradient of 0−1 M NaCl. The fusion protein eluted in a single peak and was digested overnight at 4 °C in the presence of 1% (by mass) TEV protease. The samples were loaded again onto GS4B to remove the free GST, and the proteins were collected and concentrated to ∼5 mg mL^{-1} for future assays. Phosphorylation of Rb^{NP} was achieved as previously described using 10% (by mass) purified Cdk2−CycA in a reaction containing 5 mM ATP and 20 mM $MgCl_2$.[13] After an overnight reaction at 4 °C, quantitative phosphorylation on two sites was validated by observation of an increase in molecular mass of ∼160 Da using electrospray ionization mass spectrometry (Supporting Information Figure 4). Synthetic E7 LxCxE (DLYCYEQLN), LIN52 (TDLEASLLSFEKLDRAphosSPDLWPE), cyclin D (MEHQLLCCEVETIRRAY), and TMR-$E2F2^{TD}$ (QDDYLWGLEAGEGISDLFD) peptides were ordered from Genscript, LLC.

Isothermal Titration Calorimetry. ITC experiments were performed with a VP-ITC calorimeter from Microcal, LLC (now supported by Malvern Instruments). Prior to the measurements, unphosphorylated and phosphorylated Rb^{NP} and $E2F1^{TD}$ were dialyzed overnight in the same beaker against a buffer containing 40 mM Tris, 100 mM NaCl, and 1 mM 2-mercaptoethanol (pH 8.0). Measurements were made with an $E2F1^{TD}$ concentration of 1 mM, an Rb^{NP} concentration of 15−25 μM, and an LxCxE peptide concentration of 100 μM. The reported K_d values are the average of 2−3 measurements, and the standard deviation is reported as the error.

Fluorescence Polarization Assay and Screen. Fluorescence polarization measurements were made in black, untreated 384-well plates (Corning). For the screen, 20 μL of a 40 nM solution of Rb^{NP} was dispensed using a Matrix Wellmate peristaltic pump. Compounds or DMSO were pin-transferred using a 200 nL pin tool (PerkinElmer) to a final concentration of 50 μM. Then, 20 μL of a 20 nM $E2F^{TMR}$ solution was added for a resulting final concentration of 20 nM Rb^{NP} and 10 nM $E2F^{TMR}$. All solutions were prepared using a buffer containing 40 mM Tris, 100 mM NaCl, 1 mM DTT, and 0.1% Tween-20 (pH 8.0). Total fluorescence and fluorescence polarization were measured using a PerkinElmer Envision plate reader. An excitation filter centered around a wavelength of 531 nM and with a bandwidth of 20 nM was used along with a emission filter centered around 595 nM and with a bandwidth of 60 nM. Fluorescence polarization ratios were calculated as $FP = 1000(S - G \times P)/(S + G \times P)$, where S is intensity of fluorescence parallel to excitation plane, P is perpendicular fluorescence intensity, and G is a correction factor to ensure positive ratio values. For the protein titration experiments, 10 μM of E7 LxCxE peptide, 2 μM of E7 protein, or 50 μM compound was added to prepared solutions of Rb^{NP} at the different indicated concentrations. Binding constants were determined from fits of the protein titration data using a two-site binding model, and the y intercept was fixed to the FP value of the $E2F^{TMR}$ peptide alone. Reported errors in the K_d from FP measurements are curve-fitting errors. The EC50 measurement was performed using conditions similar to the screen except 20 nM Rb^{NP} was used. We report % activity = $(FP_{phosRb+activator} - FP_{phosRb})/(FP_{unphosRb} - FP_{phosRb})$.

ASSOCIATED CONTENT

Supporting Information

The Supporting Information is available free of charge on the ACS Publications website at DOI: 10.1021/acschembio.6b00011.

Supporting Figures 1−4, Supporting Table 1 (PDF)

AUTHOR INFORMATION

Corresponding Author

*E-mail: srubin@ucsc.edu.

Notes

The authors declare no competing financial interest.

ACKNOWLEDGMENTS

This work was supported by the U.S. Army Medical Research and Materiel Command, through the Breast Cancer Research Program under Award No. W81XWH-14-1-0329 to S.M.R. Opinions, interpretations, conclusions, and recommendations are those of the author and are not necessarily endorsed by the U.S. Army. This work was also supported by grant R01CA132685 from the National Cancer Institute to S.M.R. and by the Santa Cruz Cancer Benefit Group. The high-throughput screening performed in the UCSC Chemical Screening Center was supported by NIH shared instrumentation grant 1 S10 RR022455.

REFERENCES

(1) Burkhart, D. L., and Sage, J. (2008) Cellular mechanisms of tumour suppression by the retinoblastoma gene. *Nat. Rev. Cancer 8*, 671−682.

(2) Classon, M., and Harlow, E. (2002) The retinoblastoma tumour suppressor in development and cancer. *Nat. Rev. Cancer 2*, 910−917.

(3) Dick, F. A., and Rubin, S. M. (2013) Molecular mechanisms underlying RB protein function. *Nat. Rev. Mol. Cell Biol. 14*, 297−306.

(4) Lipinski, M. M., and Jacks, T. (2000) The retinoblastoma gene family in differentiation and development. *Oncogene 18*, 7873−7882.

(5) Knudsen, E. S., and Knudsen, K. E. (2008) Tailoring to RB: tumour suppressor status and therapeutic response. *Nat. Rev. Cancer 8*, 714−724.

(6) Malumbres, M., and Barbacid, M. (2001) To cycle or not to cycle: a critical decision in cancer. *Nat. Rev. Cancer 1*, 222−231.

(7) Sherr, C. J. (1996) Cancer cell cycles. *Science 274*, 1672−1677.

(8) Stone, A., Sutherland, R. L., and Musgrove, E. A. (2012) Inhibitors of cell cycle kinases: recent advances and future prospects as cancer therapeutics. *Crit. Rev. Oncog. 17*, 175−198.

(9) Fera, D., Schultz, D. C., Hodawadekar, S., Reichman, M., Donover, P. S., Melvin, J., Troutman, S., Kissil, J. L., Huryn, D. M., and Marmorstein, R. (2012) Identification and characterization of small molecule antagonists of pRb inactivation by viral oncoproteins. *Chem. Biol. 19*, 518−528.

(10) Lee, J. O., Russo, A. A., and Pavletich, N. P. (1998) Structure of the retinoblastoma tumour-suppressor pocket domain bound to a peptide from HPV E7. *Nature 391*, 859−865.

(11) Rubin, S. M. (2013) Deciphering the retinoblastoma protein phosphorylation code. *Trends Biochem. Sci. 38*, 12−19.

(12) Lees, J. A., Buchkovich, K. J., Marshak, D. R., Anderson, C. W., and Harlow, E. (1991) The retinoblastoma protein is phosphorylated on multiple sites by human cdc2. *EMBO J. 10*, 4279−4290.

(13) Burke, J. R., Deshong, A. J., Pelton, J. G., and Rubin, S. M. (2010) Phosphorylation-induced conformational changes in the retinoblastoma protein inhibit E2F transactivation domain binding. *J. Biol. Chem. 285*, 16286−16293.

(14) Burke, J. R., Hura, G. L., and Rubin, S. M. (2012) Structures of inactive retinoblastoma protein reveal multiple mechanisms for cell cycle control. *Genes Dev. 26*, 1156−1166.

(15) Brown, V. D., Phillips, R. A., and Gallie, B. L. (1999) Cumulative effect of phosphorylation of pRB on regulation of E2F activity. *Mol. Cell. Biol. 19*, 3246−3256.

(16) Knudsen, E. S., and Wang, J. Y. (1997) Dual mechanisms for the inhibition of E2F binding to RB by cyclin-dependent kinase-mediated RB phosphorylation. *Mol. Cell. Biol. 17*, 5771−5783.

(17) Lents, N. H., Gorges, L. L., and Baldassare, J. J. (2006) Reverse mutational analysis reveals threonine-373 as a potentially sufficient phosphorylation site for inactivation of the retinoblastoma tumor suppressor protein (pRB). *Cell Cycle 5*, 1699−1707.

(18) Zhang, J. H., Chung, T. D., and Oldenburg, K. R. (1999) A Simple Statistical Parameter for Use in Evaluation and Validation of High Throughput Screening Assays. *J. Biomol. Screening 4*, 67−73.

(19) Brideau, C., Gunter, B., Pikounis, B., and Liaw, A. (2003) Improved statistical methods for hit selection in high-throughput screening. *J. Biomol. Screening 8*, 634−647.

(20) Irwin, J. J., Duan, D., Torosyan, H., Doak, A. K., Ziebart, K. T., Sterling, T., Tumanian, G., and Shoichet, B. K. (2015) An Aggregation Advisor for Ligand Discovery. *J. Med. Chem. 58*, 7076−7087.

(21) Johnston, P. A. (2011) Redox cycling compounds generate H2O2 in HTS buffers containing strong reducing reagents–real hits or promiscuous artifacts? *Curr. Opin. Chem. Biol. 15*, 174−182.

(22) Jones, R. E., Wegrzyn, R. J., Patrick, D. R., Balishin, N. L., Vuocolo, G. A., Riemen, M. W., Defeo-Jones, D., Garsky, V. M., Heimbrook, D. C., and Oliff, A. (1990) Identification of HPV-16 E7 peptides that are potent antagonists of E7 binding to the retinoblastoma suppressor protein. *J. Biol. Chem. 265*, 12782−12785.

(23) Guiley, K. Z., Liban, T. J., Felthousen, J. G., Ramanan, P., Litovchick, L., and Rubin, S. M. (2015) Structural mechanisms of DREAM complex assembly and regulation. *Genes Dev. 29*, 961−974.

(24) Fattaey, A. R., Harlow, E., and Helin, K. (1993) Independent regions of adenovirus E1A are required for binding to and dissociation of E2F-protein complexes. *Mol. Cell. Biol. 13*, 7267−7277.

(25) Patrick, D. R., Oliff, A., and Heimbrook, D. C. (1994) Identification of a novel retinoblastoma gene product binding site on human papillomavirus type 16 E7 protein. *J. Biol. Chem. 269*, 6842−6850.

(26) Zalvide, J., Stubdal, H., and DeCaprio, J. A. (1998) The J domain of simian virus 40 large T antigen is required to functionally inactivate RB family proteins. *Mol. Cell. Biol. 18*, 1408−1415.

(27) Bullock, B. N., Jochim, A. L., and Arora, P. S. (2011) Assessing helical protein interfaces for inhibitor design. *J. Am. Chem. Soc. 133*, 14220−14223.

(28) Cummings, C. G., and Hamilton, A. D. (2010) Disrupting protein-protein interactions with non-peptidic, small molecule alpha-helix mimetics. *Curr. Opin. Chem. Biol. 14*, 341−346.

(29) Grasberger, B. L., Lu, T., Schubert, C., Parks, D. J., Carver, T. E., Koblish, H. K., Cummings, M. D., LaFrance, L. V., Milkiewicz, K. L., Calvo, R. R., Maguire, D., Lattanze, J., Franks, C. F., Zhao, S., Ramachandren, K., Bylebyl, G. R., Zhang, M., Manthey, C. L., Petrella, E. C., Pantoliano, M. W., Deckman, I. C., Spurlino, J. C., Maroney, A. C., Tomczuk, B. E., Molloy, C. J., and Bone, R. F. (2005) Discovery and cocrystal structure of benzodiazepinedione HDM2 antagonists that activate p53 in cells. *J. Med. Chem. 48*, 909−912.

(30) Vassilev, L. T., Vu, B. T., Graves, B., Carvajal, D., Podlaski, F., Filipovic, Z., Kong, N., Kammlott, U., Lukacs, C., Klein, C., Fotouhi, N., and Liu, E. A. (2004) In vivo activation of the p53 pathway by small-molecule antagonists of MDM2. *Science 303*, 844−848.

DOI: 10.1021/acschembio.6b00911